

Article

Not peer-reviewed version

Hydrazine Oxidation in Aqueous Solutions I. N₄H₆ Decomposition

[Martin Breza](#)^{*} and Alena Manova

Posted Date: 1 October 2023

doi: 10.20944/preprints202310.0008.v1

Keywords: Coupled Cluster; geometry optimization; N-N bond splitting; QTAIM analysis; electron structure



Preprints.org is a free multidiscipline platform providing preprint service that is dedicated to making early versions of research outputs permanently available and citable. Preprints posted at Preprints.org appear in Web of Science, Crossref, Google Scholar, Scilit, Europe PMC.

Copyright: This is an open access article distributed under the Creative Commons Attribution License which permits unrestricted use, distribution, and reproduction in any medium, provided the original work is properly cited.

Article

Hydrazine Oxidation in Aqueous Solutions I. N_4H_6 Decomposition

Martin Breza ^{1,*} and Alena Manova ²

¹ Dept. Physical Chemistry, Slovak Technical University, Radlinskeho 9, SK-81237 Bratislava, Slovakia; marti.breza@stuba.sk

² Dept. Analytical Chemistry, Slovak Technical University, Radlinskeho 9, SK-81237 Bratislava, Slovakia; alena.manova@stuba.sk; e-mail@e-mail.com

* Correspondence: martin.breza@stuba.sk

Abstract: A mixture of nonlabeled ($^{14}N_2H_4$) and ^{15}N labeled hydrazine ($^{15}N_2H_4$) in an aqueous solution is oxidized to $^{15}N_2$, $^{14}N_2$ and $^{14}N^{15}N$ molecules, indicating the intermediate existence of the $^{14}NH_2-^{14}NH-^{15}NH-^{15}NH_2$ with subsequent hydrogen transfers and splitting of side N-N bonds. Structures, thermodynamics, and electron characteristics of various N_4H_6 molecules in aqueous solutions are investigated using theoretical treatment at the CCSD/cc-pVTZ level of theory to explain the crucial part of the hydrazine oxidation reaction. Most N_4H_6 structures in aqueous solutions are decomposed during geometry optimization. Splitting the bond between central nitrogen atoms is the most frequent, but the breakaway of the side nitrogen is energetically the most preferred. The N-N fissions are enabled by suitable hydrogen rearrangements. Gibbs free energy data indicate the dominant abundance of $NH_3 \dots N_2 \dots NH_3$ species. The side N atoms have very high negative charges, which should support hydrogen transfers in aqueous solutions. The only stable cyclo-(NH)₄...H₂ structure has a too high Gibbs energy and breaks the H₂ molecule. The remaining initial cyclic structures are split into hydrazine and HN=NH or H₂N=N species, and their relative abundance in aqueous solutions is vanishing.

Keywords: Coupled Cluster; geometry optimization; N-N bond splitting; QTAIM analysis; electron structure

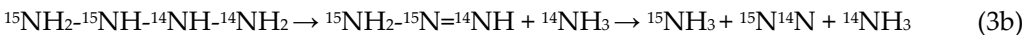
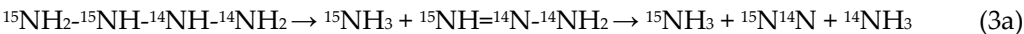
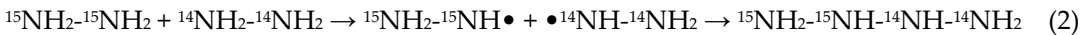
1. Introduction

Hydrazine N_2H_4 is a colorless flammable liquid that is used in industry and agriculture due to its reducing properties. It is used as a corrosion inhibitor in boilers, as a rocket propellant, antioxidant, catalyst, and pesticide precursor. In boiler water, it serves as an oxygen scavenger that reacts with oxygen into nitrogen and water only, which does not cause corrosion of ferrous metals. Unreacted hydrazine can be decomposed into ammonia, which can be corrosive to copper and copper-containing alloys [1]. Thus the knowledge of the exact mechanism of its oxidation is of practical importance so far.

Higginson and Sutton [2] studied the oxidation of ^{15}N -enriched hydrazine by an excess of various oxidizing agents in aqueous solutions. Mass spectroscopic analysis of the evolved nitrogen for 28, 29, and 30 mass-number abundance (i.e. incidence of $^{14}N_2$, $^{15}N^{14}N$ and $^{15}N_2$ molecules, respectively) has shown that the proportion of $^{15}N_2$ molecules decreased while that of $^{15}N^{14}N$ molecules increased depending on the oxidizing agent used. If the nitrogen produced by the reaction



involves no N-N fission, the evolved N_2 molecule originates in the same N_2H_4 molecule, and therefore it must have the same distribution of ^{15}N isotopes as the hydrazine reactant. This implies that some of the nitrogen molecules are formed by a mechanism involving a N-N fission and the formation of nitrogen-containing radicals from two different hydrazine molecules as follows:



Cahn and Powell [3] confirmed the randomized $^{15}\text{N}^{14}\text{N}$ composition obtained by one-electron oxidation of ^{15}N enriched hydrazines with a number of oxidizing agents unlike exclusively four-electron oxidizing agents (acid iodate, alkaline ferricyanide) that produced unrandomized N_2 molecules (all four hydrogen atoms must be removed from a single hydrazine molecule). Petek and Bruckenstein [4] observed that the electrooxidation of ^{15}N labelled hydrazine (96.7% enrichment) at Pt electrode produced N_2 molecules with the ratio of $^{14}\text{N}^{15}\text{N}/^{15}\text{N}^{15}\text{N} = 0.07\pm0.01$ while in Ce(IV) solutions it was 0.9 ± 0.2 . A ratio of both isotopic forms between these two limits was produced by simultaneous electrooxidation and homogeneous oxidation with electrogenerated Ce(IV).

A bright yellow substance, stable under $-178\text{ }^\circ\text{C}$, is formed after thermal decomposition of hydrazine at high temperatures and low pressures in a flowing system [5]. The authors suppose that it is tetrazane N_4H_6 .

Based on polarographic and voltammetric studies of hydrazine in alkali solutions, Karp and Meites [6] suggested its two-electron oxidation to diimide with subsequent dimerization and decomposition as follows



The proposed mechan(3)ism is also capable of explaining the randomized $^{15}\text{N}^{14}\text{N}$ composition.

Ball [7] investigated the structure and some thermochemical properties of the cis- and trans-conformations of tetrazane $\text{NH}_2\text{-NH-NH-NH}_2$ using various-level ab initio methods. Unlike nearly planar trans-conformation, the cis-conformation should be denoted as a gauche structure (N-N-N-N dihedral angle of ca 90°).

The decomposition of hydrazine was studied at CCSD(T)-F12a/aug-ccpVTZ// ω B97x-D3/6-311++G(3df,3pd) level of theory [8]. A comprehensive analysis of the N_4H_6 singlet potential energy surfaces was performed. Three stable isomers $\text{NH}_2\text{-NH-NH-NH}_2$, $\text{NH}_2\text{-NH-NH}_2=\text{NH}$ and $\text{NH}_2\text{-NH}_2\text{-N}=\text{NH}_2$ and the transition states for H transfers between them were obtained as well. Stabilized $\text{NH}_2\text{-NH-NH-NH}_2$ formation becomes significant only at relatively high pressures and low temperatures due to decomposition into $\text{N}_2\text{H}_3\bullet + \text{N}_2\text{H}_3\bullet$. No direct reaction between $\text{NH}_2\text{-NH-NH-NH}_2$ and $\text{NH}_2\text{-NH}_2\text{-N-NH}_2$ was found. NH_3 eliminations from $\text{NH}_2\text{-NH-NH-NH}_2$ and $\text{NH}_2\text{-NH}_2\text{-N-NH}_2$ are energetically preferred, but only $\text{NH}_2\text{-NH}_2\text{-N}=\text{NH}_2$ has relatively small activation energy for this reaction (see Table 1).

Table 1. Reaction, ΔE_r , and activation, E_a , energy data of elementary reactions on the N_4H_6 potential energy surface [8].

Reaction	ΔE_r (kJ/mol)	E_a (kJ/mol)
$\text{N}_2\text{H}_4 + \text{H}_2\text{N}=\text{N} \rightarrow \text{NH}_2\text{-NH-NH-NH}_2$	-103.6	50.6
$\text{N}_2\text{H}_4 + \text{H}_2\text{N}=\text{N} \rightarrow \text{NH}_2\text{NH}_2\text{N}=\text{NH}_2$	29.0	55.4
$\text{NH}_2\text{-NH-NH-NH}_2 \rightarrow \text{NH}_2\text{NH}=\text{N} + \text{NH}_3$	7.5	178.7
$\text{NH}_2\text{-NH-NH-NH}_2 \rightarrow \text{NH}_2\text{-N}=\text{NH} + \text{NH}_3$	-102.5	214.1
$\text{NH}_2\text{-NH}_2\text{-N}=\text{NH}_2 \rightarrow \text{NH}_2\text{-N}=\text{NH} + \text{NH}_3$	-245.1	38.7
$\text{NH}_2\text{-NH-NH-NH}_2 \rightarrow \text{NH}_2\text{-NH-NH}_2=\text{NH}$	151.1	158.6
$\text{NH}_2\text{-NH-NH}_2=\text{NH} \rightarrow \text{NH}_2\text{-NH}_2\text{-N}=\text{NH}_2$	-18.5	74.4
$\text{N}_2\text{H}_3\bullet + \text{N}_2\text{H}_3\bullet \rightarrow \text{NH}_2\text{-NH-NH-NH}_2$	-152.9	0.2
$\text{NH}_2\text{-NH}=\text{NH}\bullet + \text{NH}_2\bullet \rightarrow \text{NH}_2\text{-NH-NH-NH}_2$	208.9	0.2
$\text{NH}=\text{NH}_2\text{-NH}\bullet + \text{NH}_2\bullet \rightarrow \text{NH}_2\text{-NH-NH}_2=\text{NH}$	682.7	0.2



It is evident that the N₄H₆ decomposition is crucial for the hydrazine oxidation with subsequent ¹⁵N¹⁴N molecules formation. It depends on the suitable N₄H₆ site of N-N bond splitting. At first, the NH₂-NH-NH-NH₂ isomer is formed by the reaction



In the next steps, H transfers and possible N-N bond splitting may proceed. The main aim of this study is a quantum-chemical study of N₄H₆ isomers in aqueous solutions at the solely Coupled Cluster level of theory and to determine the sites of the possible N-N fission in them. The thermodynamic properties of the decomposition reaction products enable us to predict the possible formation of ¹⁵N¹⁴N molecules in real systems. The electronic structure of the optimized structures will also be discussed.

2. Results and discussion

We consider possible linear isomers of N₄H₆ with the N1-N2-N3-N4 backbone and the composition N1H_m-N2H_n-N3H_p-N4H_q, where subscripts m, n, p, q denote the number of H atoms bonded to individual Ni, i = 1 → 4, atoms, and m + n + p + q = 6. We started geometry optimizations from anti- and syn-conformations of N1-N2-N3-N4. The optimized structures usually correspond to gauche-conformers or some N-N bonds are split (see Table 2). If N1 and N2 correspond to ¹⁵N atoms while N3 and N4 correspond to the ¹⁴N ones, then N1-N2 and N3-N4 fissions would lead to ¹⁵N¹⁴N molecules, unlike the N2-N3 fissions.

In the case of cyclo-N₄H₆ isomers we can use the same notation, but any N-N fission can lead to ¹⁵N¹⁴N molecules because of suitable H transfers within the cycle.

Table 2. N1-N2-N3-N4 dihedral angles (Θ₁₂₃₄), absolute (G₂₉₈) and relative (ΔG₂₉₈) Gibbs free energies at 298.15 K of the optimized N₄H₆ structures obtained from the starting ones. The most stable structure is highlighted in bold.

Starting	Optimized	Θ ₁₂₃₄ [°]	G ₂₉₈ [Hartree]	ΔG ₂₉₈ [kJ/mol]	Remarks
A2112	D2112a	168.3	-222.09177	0.00	
A2121	D2121a	-161.4	-222.04654	118.75	
A2211	E(22)(11)a	-33.7	-222.10760	-41.56	H ₂ N-NH ₂ + HN=NH
A2202	A2202	-179.9	-222.04618	119.71	
A2220	E(22)(20)a	146.5	-222.07817	35.7	H ₂ N-NH ₂ + H ₂ N=N
A1221	D1221	-168.5	-222.00357	231.58	
A3210	E(32)(10)	14.3	-222.04629	119.42	H ₃ N-NH ₂ + HN=N
A3201	E(22)(11)b	-142.8	-222.10755	-41.43	H ₂ N-NH ₂ + HN=NH, 1→3 H rearrangement
A3201	E(3)(201)b	-26.5	-222.1489	-150.04	NH ₃ + H ₂ N-N=NH
A3111	D2112b	75.6	-222.09311	-3.52	1→4 H rearrangement
A3120	E(31)(20)	-21.4	-222.03229	156.16	H ₃ N-NH + H ₂ N=N
A3102	E(3)(102)a	-177.1	-222.14926	-150.94	NH ₃ + HN=N-NH ₂
A3012	D3012a	88.8	-222.04832	114.07	
A3021	A3021	176.8	-221.99866	244.46	
A3003	E(3)(00)(3)	60.4	-222.26295	-449.44	2NH ₃ + N ₂
B2112	D2112c	72.0	-222.09665	-12.80	
B2121	D2121b	-65.0	-222.04530	122.02	

B2121	D2121c	-44.8	-222.04982	110.13	
B2211	E(22)(11)a	-33.7	-222.10760	-41.56	H ₂ N-NH ₂ + HN=NH
B2202	D2202a	73.7	-222.05056	108.21	
B2220	E(22)(20)b	-32.9	-222.07820	35.64	H ₂ N-NH ₂ + H ₂ N=N
B1221	F12)(21	75.8	-222.09760	-15.30	N2-N3 fission, N1-N4 bonding
B1221	F1)(22)(1	-33.3	-222.10756	-41.45	H ₂ N-NH ₂ + HN=NH, N1-N4 bonding
B3210	E(22)(11)c	-34.0	-222.10754	-41.41	H ₂ N-NH ₂ + HN=NH, 1→4 H rearrangement
B3201	D2202b	80.1	-222.04758	116.02	1→4 H rearrangement
B3201	E(3)(201)	-26.5	-222.14892	-150.04	NH ₃ + H ₂ N=N-NH
B3111	D2112b	75.6	-222.09311	-3.52	1→4 H rearrangement
B3120	D2121d	68.8	-222.04651	118.82	1→4 H rearrangement
B3102	E(3)(102)b	-20.6	-222.14678	-144.42	NH ₃ + HN=N-NH ₂
B3012	D3012b	-59.7	-222.04910	112.02	
B3021	D2022	-73.8	-222.05056	108.21	1→4 H rearrangement
B3003	E(3)(00)(3)	60.4	-222.26235	-449.44	2 NH ₃ + N ₂
C2211	E(22)(11)d	12.3	-222.10759	-41.45	H ₂ N-NH ₂ + HN=NH
C2202	E(22)(02)	29.6	-222.07822	35.58	H ₂ N-NH ₂ + N=NH ₂
C2121	E1111	23.1	-221.99631	250.64	Cyclo-N ₄ H ₄ + H ₂

We introduce the notation X_{mnpq} for individual systems under study, where X = A, B, C, and D stands for anti-, syn-, cyclic, and gauche-structures and the indices m, n, p, and q are explained above. X = E denotes structures with N-N fissions, i.e., consisting of two or three molecules after geometry optimization. X = F stands for structures with N2-N3 fissions and subsequent N1-N4 bond formations. The N-N fissions in E and F systems are denoted by round brackets where the mutually bonded N atoms are included in the same bracket couple. The different structures with the same X_{mnpq} notation can be distinguished by additional letters a, b, c, etc. For example, E(22)(11)a and E(22)(11)b denote two different structures composed of H₂N-NH₂ and HN=NH molecules.

The N₄H₆ structures under study are in Table 2 divided into three groups according to the initial N1-N2-N3-N4 conformations. The H atom rearrangements during geometry optimizations are less frequent in the anti-conformations (starting A structures) than in the syn-conformations (starting B structures). In both groups the probability of N-N fissions is approximately 50%, and N2-N3 fissions prevail. On the other hand, the N1-N2 fissions lead to energetically much more preferred products such as E(3)(201), E(3)(102) and especially E(3)(00)(3). In the B1221 syn-conformation the mutual interaction of N1 and N4 causes the formation of the N1-N4 bond and N2-N3 fission leading to the structure of H₂N2-N1H-N4H-N3H₂, i.e. F12)(21, in gauche-conformation or decomposition to more stable HN1=N4H and the H₂N2-N3H₂ species denoted as the F1)(22)(1 system.

The relative Gibbs free energies in Table 2 are related to the structure D2112a obtained by the reaction (5) in the first step. According to these data, the system E(3)(00)(3), which corresponds to ¹⁵NH₃, ¹⁴NH₃ and ¹⁵N¹⁴N molecules, is dominant among all N₄H₆ structures in aqueous solutions under normal conditions and the relative abundance of the remaining systems is vanishing. In general, the decomposed E systems are more stable than the remaining structures (see Tables 2–4, Figures 1 and 2).

During the geometry optimization of the starting cyclic C structures (Table 2), only the least stable cyclo-(NH)₄ structure, denoted as E1111, preserves its tetraatomic ring after removing a H₂ molecule. The remaining C structures split into hydrazine and HN=NH in E(22)(11)d or H₂N=N in E(22)(02). The disadvantage of cyclic structure preservation is indicated by preferring the above-mentioned F structures after N1-N4 bonding within geometry optimization of the starting B1221 syn-conformation.

Table 3. Interatomic distances (in Å) in the optimized Amnpq and Dmnpq structures.

Structure	N1-N2	N2-N3	N3-N4	N1-H	N2-H	N3-H	N4-H
D1221	1.341	1.840	1.338	1.017	1.019	1.015	1.018
					1.016	1.021	
D2112a	1.423	1.467	1.431	1.012	1.014	1.016	1.011
				1.018			1.014
D2112b	1.432	1.419	1.440	1.012	1.018	1.013	1.011
				1.015			1.015
D2112c	1.424	1.428	1.437	1.013	1.016	1.014	1.011
				1.017			1.015
D2121a	1.413	1.480	1.412	1.011	1.015	1.020	1.018
				1.017		1.021	
D2121b	1.423	1.467	1.417	1.010	1.018	1.017	1.019
				1.013		1.020	
D2121c	1.413	1.504	1.409	1.013	1.017	1.017	1.020
				1.024		1.020	
D2121d	1.423	1.467	1.415	1.010	1.018	1.016	1.018
				1.013		1.021	
A2202	1.427	1.454	1.443	1.016(2×)	1.021(2×)	-	1.013(2×)
D2202a	1.459	1.422	1.446	1.017(2×)	1.016	-	1.012
					1.022		1.013
D2202b	1.464	1.418	1.446	1.016	1.017	-	1.012
				1.018	1.021		1.014
D2022	1.459	1.421	1.447	1.017(2×)	1.016	-	1.012
					1.022		1.013
A3021	1.463	1.452	1.433	1.016	-	1.020	1.019
				1.024(2×)		1.025	
D3012a	1.463	1.418	1.463	1.016	-	1.013	1.015
				1.021(2×)			1.017
D3012b	1.493	1.395	1.485	1.014	-	1.021	1.014
				1.021(2×)			1.017

Table 4. Interatomic distances (in Å) in the optimized Emnpq and Fmnpq systems.

System	N1-N2	N2-N3	N3-N4	N1-H	N2-H	N3-H	N4-H
E1111 ^{a)}	1.476	1.481	1.481	1.023	1.017	1.017	1.017
E(22)(11)a	1.446	3.118	1.245	1.012	1.011	1.030	1.027
				1.014	1.014		
E(22)(11)b	1.446	3.465	1.245	1.011	1.012	1.030	1.027
				1.014	1.014		
E(22)(11)c	1.445	3.292	1.245	1.011	1.012	1.027	1.030
				1.014	1.014		
E(22)(11)d	1.446	3.116	1.245	1.012	1.011	1.030	1.027
				1.014	1.014		
E(22)(20)a	1.446	3.271	1.225	1.011	1.013	1.028	-
				1.014	1.014	1.034	
E(22)(20)b	1.446	2.971	1.225	1.013	1.011	1.028	-
				1.014	1.014	1.033	
E(22)(02)	1.447	3.276	1.225	1.011	1.013	-	1.028
				1.014	1.014		1.033
E(31)(20)	1.468	2.750	1.230	1.018(2×)	1.016	1.029	-
				1.029		1.057	
E(32)(10)	1.445	3.035	1.242	1.018(2×)	1.015	1.076	-
				1.021	1.079		
E(3)(201)	3.088	1.350	1.249	1.013(3×)	1.006	-	1.019
					1.022		
E(3)(102)a	3.117	1.243	1.365	1.013(3×)	1.026	-	1.008
							1.014
E(3)(102)b	3.760	1.246	1.356	1.013(2×)	1.032	-	1.007
				1.014			
E(3)(00)(3)	3.636	1.096	3.711	1.014(3×)	-	-	1.013(3×)
F(11)(22)	1.245	3.291	1.446	1.030	1.027	1.012	1.011
						1.014	1.014
F12)(21 ^{b)}	1.430	3.017	1.424	1.012	1.012	1.012	1.017
					1.018	1.017	

Remarks: ^{a)}N1-N4 bond length of 1.476 Å; ^{b)}N1-N4 bond length of 1.432 Å.

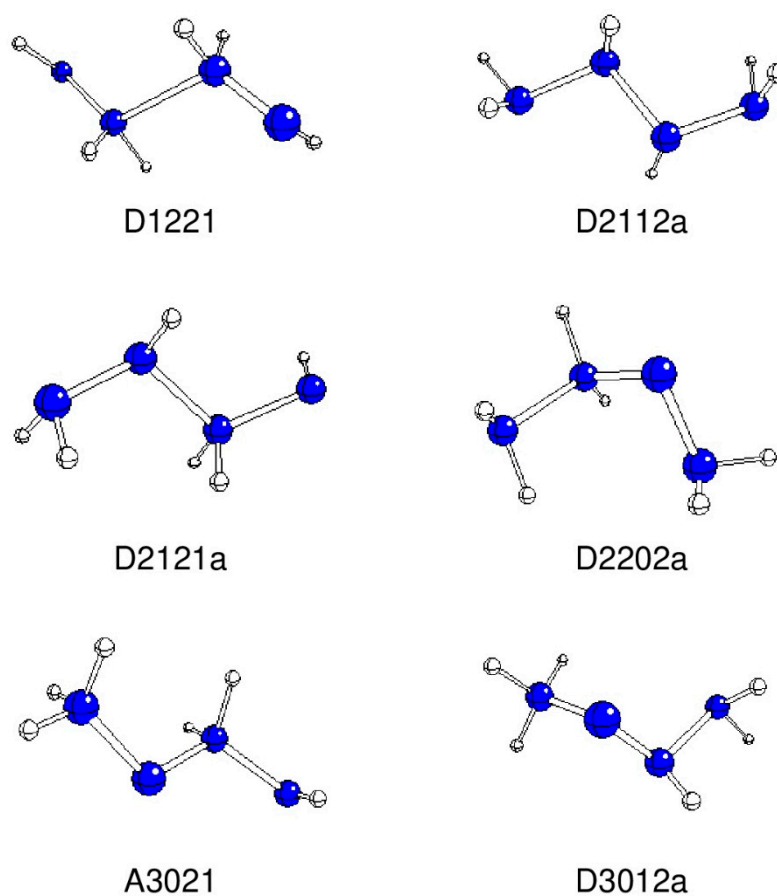


Figure 1. Optimized geometries of stable A and D structures (N – blue, H – white).

The bonding in N_4H_6 structures can be described by individual bond lengths d (Tables 3 and 4) as well as by the corresponding electron density ρ (Tables 5 and 6) and ellipticity ϵ (Tables 7 and 8) at their bond critical points BCP [9]. Bond strengths decrease with bond lengths d and increase with their BCP electron densities ρ_{BCP} . Their double bond character in acyclic structures increases with their BCP ellipticities ϵ_{BCP} .

The D1221 structure has an extremely long N2-N3 bond and the remaining N-N bonds are shorter than the average N_4H_6 . The $\rho_{BCP}(N2-N3) \sim 0.1 \text{ e/bohr}^3$ corresponds to a very weak bond, the remaining N-N bonds are approximately three times stronger. The $\epsilon_{BCP}(N2-N3) \sim 0.1$ is relatively high, and the remaining double N-N bonds have a ca double ellipticity.

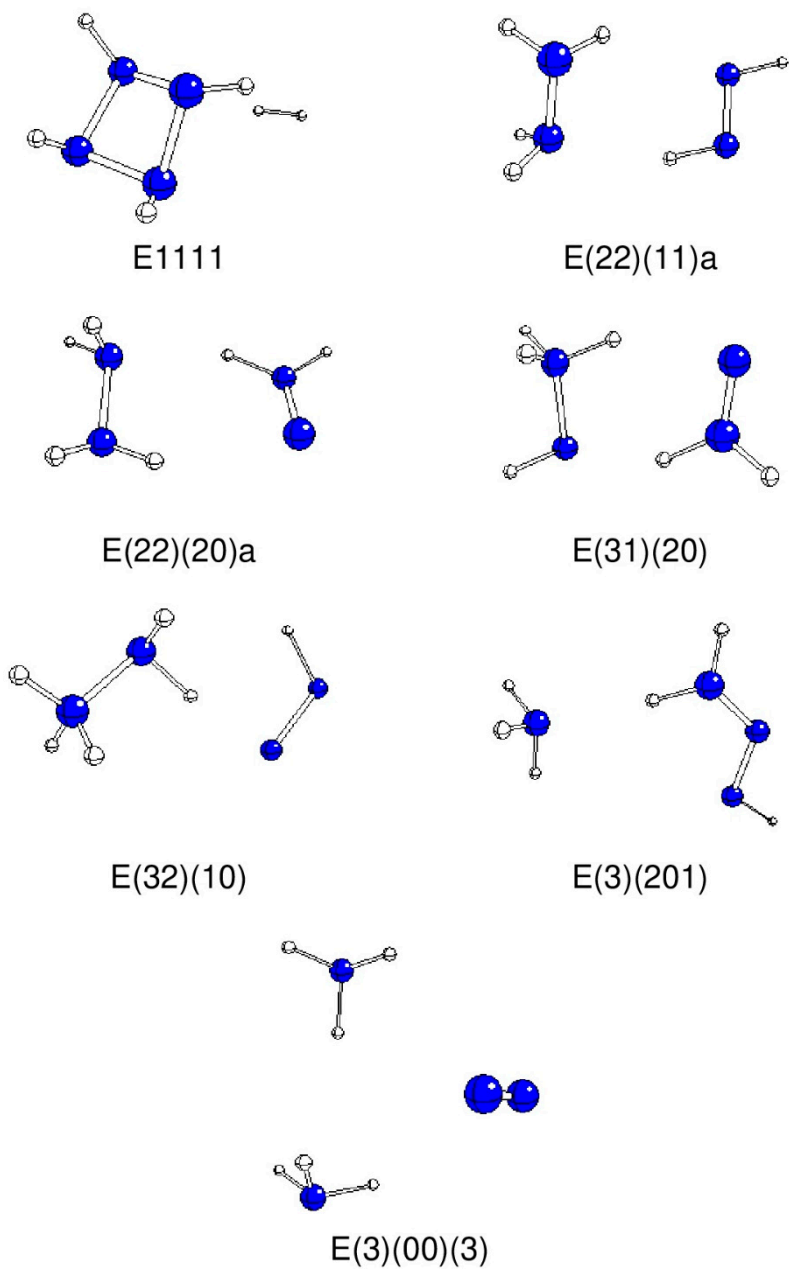


Figure 2. Optimized geometries of stable E systems (N – blue, H – white).

Table 5. BCP electron density (in e/bohr³) of N-N and N-H bonds in the optimized Amnpq and Dmnpq structures.

Structure	N1-N2	N2-N3	N3-N4	N1-H	N2-H	N3-H	N4-H
D1221	0.3705	0.1281	0.3734	0.3450	0.3483	0.3467	0.3448
					0.3528	0.3534	
D2112a	0.3156	0.2911	0.3092	0.3459	0.3574	0.3551	0.3492
				0.3515			0.3518
D2112b	0.3092	0.3237	0.3036	0.3494	0.3527	0.3561	0.3484
				0.3508			0.3514

D2112c	0.3149	0.3165	0.3050	0.3472	0.3542	0.3552	0.3484
				0.3513			0.3515
D2121a	0.3212	0.2827	0.3080	0.3458	0.3544	0.3520	0.3415
				0.3516		0.3527	
D2121b	0.3149	0.2920	0.3074	0.3509	0.3524	0.3521	0.3404
				0.3517		0.3551	
D2121c	0.3224	0.2668	0.3133	0.3406	0.3542	0.3508	0.3404
				0.3505		0.3556	
D2121d	0.3149	0.2928	0.3086	0.3503	0.3523	0.3509	0.3417
				0.3521		0.3559	
A2202	0.3148	0.2864	0.2965	0.3478(2×)	0.3514(2×)	-	0.3504
							0.3503
D2202a	0.2928	0.3098	0.2951	0.3469	0.3499	-	0.3506(2×
				0.3474	0.3553)
D2202b	0.2898	0.3107	0.2956	0.3447	0.3507	-	0.3501
				0.3478	0.3549		0.3510
D2022	0.2949	0.3102	0.2930	0.3505	-	0.3498	0.3470
				0.3507		0.3552	0.3474
A3021	0.2759	0.2964	0.2956	0.3431	-	0.3499	0.3397
				0.3437		0.3542	
				0.3480			
D3012a	0.2761	0.3196	0.2874	0.3454	-	0.3564	0.3463
				0.3473			0.3476
				0.3500			
D3012b	0.2562	0.3362	0.2736	0.3446	-	0.3488	0.3455
				0.3450			0.3497
				0.3501			

Table 6. BCP electron density (in e/bohr³) of N-N and N-H bonds in the optimized Emnpq and Fmnpq systems.

System	N1-N2	N2-N3	N3-N4	N1-H	N2-H	N3-H	N4-H
E1111 ^{a)}	0.2858	0.2828	0.2824	0.3506	0.3545	0.3566	0.3546
E(22)(11)a	0.2953	-	0.4863	0.3502	0.3500	0.3463	0.3483
				0.3529	0.3529		
E(22)(11)b	0.2953	-	0.4826	0.3500	0.3502	0.3462	0.3482
				0.3529	0.3529		
E(22)(11)c	0.2954	-	0.4863	0.3500	0.3503	0.3482	0.3462
				0.3529	0.3529		
E(22)(11)d	0.2953	-	0.4863	0.3502	0.3500	0.3463	0.3482
				0.3529	0.3529		
E(22)(20)a	0.2947	-	0.4970	0.3499	0.3501	0.3367	-
				0.3529	0.3518	0.3422	

E(22)(20)b	0.2945	-	0.4967	0.3501	0.3499	0.3367	-
				0.3517	0.3529	0.3423	
E(22)(02)	0.2945	-	0.4967	0.3500	0.3501	-	0.3367
				0.3529	0.3517		0.3423
E(31)(20)	0.2696	-	0.4927	0.3382	0.3426	0.3123	-
				0.3486		0.3412	
				0.3493			
E(32)(10)	0.2929	-	0.4831	0.3471	0.2909	0.3032	-
				0.3453	0.3485		
				0.3474			
E(3)(201)	-	0.3794	0.4825	0.3434	0.3531	-	0.3503
				0.3435	0.3368		
				0.3436			
E(3)(102)a	-	0.4891	0.3669	0.3435(2×)	0.3448	-	0.3457
				0.3436			0.3521
E(3)(102)b	-	0.4833	0.3719	0.3432	0.3375	-	0.3345
				0.3435			0.3523
				0.3436			
E(3)(00)(3)	-	0.7140	-	0.3432	-	-	0.3435
				0.3433			0.3437
				0.3433			0.3442
F(11)(22)	0.4863	-	0.2954	0.3463	0.3482	0.3502	0.3500
						0.3529	0.3529
F12)(21 ^b)	0.3096	-	0.3150	0.3573	0.3451	0.3470	0.3522
					0.3515	0.3515	

Remarks: ^a)N1-N4 BCP electron density of 0.2858 e/bohr³; ^b)N1-N4 BCP electron density of 0.3134 e/bohr³.

Table 7. BCP ellipticity of N-N and N-H bonds in the optimized Amnpq and Dmnpq structures.

Structure	N1-N2	N2-N3	N3-N4	N1-H	N2-H	N3-H	N4-H
D1221	0.230	0.107	0.231	0.048	0.015	0.015	0.047
					0.017	0.016	
D2112a	0.003	0.149	0.024	0.045	0.041	0.036	0.046
				0.050			0.051
D2112b	0.040	0.039	0.012	0.046	0.043	0.051	0.047
				0.051			0.051
D2112c	0.027	0.046	0.015	0.044	0.047	0.050	0.046
				0.047			0.050
D2121a	0.027	0.123	0.198	0.048	0.046	0.007	0.073
				0.051		0.009	
D2121b	0.035	0.070	0.182	0.045	0.034	0.011	0.074
				0.049		0.015	
D2121c	0.026	0.074	0.192	0.039	0.038	0.013(2×)	0.071

				0.048			
D2121d	0.025	0.069	0.178	0.045	0.033	0.012	0.073
				0.050		0.013	
A2202	0.060	0.302	0.089	0.036(2×)	0.008(2×)	-	0.055(2×)
D2202a	0.045	0.288	0.084	0.034	0.012	-	0.053(2×)
				0.035	0.013		
D2202b	0.086	0.301	0.087	0.039	0.010	-	0.052
				0.041	0.082		0.053
D2022	0.084	0.288	0.046	0.052	-	0.012	0.034
				0.053		0.013	0.035
A3021	0.268	0.222	0.169	0.106	-	0.006	0.079
				0.108		0.009	
				0.005			
D3012a	0.267	0.124	0.064	0.006	-	0.049	0.044
				0.007			0.048
				0.008			
D3012b	0.248	0.113	0.123	0.004	-	0.051	0.038(2×)
				0.005(2×)			

Table 8. BCP ellipticity of N-N and N-H bonds in the optimized Emnpq and Fmnpq systems.

System	N1-N2	N2-N3	N3-N4	N1-H	N2-H	N3-H	N4-H
E1111 ^a)	0.103	0.108	0.108	0.029	0.030	0.027	0.030
E(22)(11)a	0.008	-	0.189	0.047	0.046	0.004	0.004
				0.049	0.050		
E(22)(11)b	0.008	-	0.189	0.046	0.047	0.004	0.004
				0.050	0.049		
E(22)(11)c	0.008	-	0.189	0.046	0.047	0.004	0.004
				0.050	0.049		
E(22)(11)d	0.008	-	0.189	0.047	0.046	0.004	0.004
				0.049	0.049		
E(22)(20)a	0.008	-	0.021	0.046	0.047(2×)	0.035	-
				0.049		0.038	
E(22)(20)b	0.007	-	0.020	0.047(2×)	0.046	0.035	-
					0.049	0.038	
E(22)(02)	0.007	-	0.020	0.046	0.047(2×)	-	0.035
				0.049			0.039
E(31)(20)	0.156	-	0.005	0.006	0.080	0.029	-
				0.011		0.035	
				0.012			
E(32)(10)	0.089	-	0.072	0.009	0.027	0.005	-
				0.010(2×)	0.045		
E(3)(201)	-	0.138	0.229	0.033(3×)	0.043	-	0.008

					0.053		
E(3)(102)a	-	0.218	0.118	0.326	0.005	-	0.047
				0.327(2×)			0.051
E(3)(102)b	-	0.238	0.133	0.324(2×)	0.001	-	0.041
				0.329			0.052
E(3)(00)(3)	-	0.000	-	0.033	-	-	0.033(3×)
				0.034(2×)			
F(11)(22)	0.189	-	0.008	0.004	0.004	0.047	0.046
						0.049	0.050
F12)(21 ^b)	0.012	-	0.031	0.054	0.046	0.045	0.049
					0.051	0.047	

Remarks: ^a)N1-N4 BCP ellipticity of 0.103; ^b)N1-N4 BCP ellipticity of 0.041.

The D2112a-c structures differ in N1-N2-N3-N4 dihedral angles, and their bond length alternation decreases with non-planarity of their backbone. Their $q_{\text{BCP}}(\text{N-N})$ values vary about ~ 0.3 e/bohr³ as in single N-N bonds. The $\epsilon_{\text{BCP}}(\text{N2-N3})$ values decrease with non-planarity (~ 0.1 and less), while they are very small for the remaining N-N bonds, which correspond to single bonds.

Similarly, the D2121a-d structures differ in the N1-N2-N3-N4 dihedral angles, with the N2-N3 bond length being longer and weaker than the remaining ones. The $q_{\text{BCP}}(\text{N-N})$ values varying about ~ 0.3 e/bohr³ correspond to single N-N bonds. The $\epsilon_{\text{BCP}}(\text{N2-N3})$ values decrease with non-planarity (~ 0.1 and less), $\epsilon_{\text{BCP}}(\text{N3-N4}) \sim 0.2$ is typical for double bonds.

The N-N bond properties in the A2202, D2202a-b, and D2022 structures (aside from reverse numbering of N atoms) vary with the N1-N2-N3-N4 dihedral angles. The N2-N3 bonds are the shortest in all these systems. The $q_{\text{BCP}}(\text{N-N})$ values varying about ~ 0.3 e/bohr³ typical for single N-N bonds but the $\epsilon_{\text{BCP}}(\text{N2-N3}) \sim 0.3$ in all structures indicate a double bond character of this bond.

In A3021 the N-N bond lengths decrease with the distance from N1, and the BCP ellipticity values indicate the same trend in decreasing double bond character. However, the $q_{\text{BCP}}(\text{N-N})$ values about 0.3 e/bohr³ correspond to single N-N bonds.

Analogous trends are observed for D3012a-b structures.

In E1111 with N-N bond lengths of ca 1.5 Å and $q_{\text{BCP}}(\text{N-N}) \sim 0.3$ e/bohr³ typical for single N-N bonds, the $\epsilon_{\text{BCP}}(\text{N-N})$ values 0.108 can be explained by mechanical strain in its four-membered ring rather than by its double bond character.

The remaining E systems consist of two or three independent molecules, interacting through weak hydrogen bonds only, which can be treated independently of their parent E structures. The possible biradical character of E(32)(10) can be excluded on the basis of its atomic charges (see later) which indicate the existence of $[\text{NH}_3\text{-NH}_2]^+$ and $[\text{HN}\equiv\text{N}]^-$ charged species.

$\text{H}_2\text{N-NH}_2$ with the N-N distance of 1.45 Å, $q_{\text{BCP}}(\text{N-N}) = 0.295$ e/bohr³ and $\epsilon_{\text{BCP}}(\text{N-N}) = 0.008$ in all E systems is typical for a single N-N bonding.

HN=NH with N-N distance of 1.245 Å, $q_{\text{BCP}}(\text{N-N}) = 0.486$ e/bohr³ and $\epsilon_{\text{BCP}}(\text{N-N}) = 0.189$ in all systems E correspond to double N-N bonds.

Its isomer $\text{H}_2\text{N=N}$ has a N-N distance of 1.23 Å and $q_{\text{BCP}}(\text{N-N}) = 0.497$ e/bohr³ which correspond to the double N-N bond in contradiction with $\epsilon_{\text{BCP}}(\text{N-N}) = 0.020$.

On the other hand, $\text{NH}_3\text{-NH}$ has a N-N distance of 1.47 Å and $q_{\text{BCP}}(\text{N-N}) = 0.27$ e/bohr³, which correspond to the single N-N bond in contradiction to the high $\epsilon_{\text{BCP}}(\text{N-N})$ value of 0.156.

The $[\text{NH}_3\text{-NH}_2]^+$ cation with the N-N distance of 1.446 Å, $q_{\text{BCP}}(\text{N-N}) = 0.293$ e/bohr³ and $\epsilon_{\text{BCP}}(\text{N-N}) = 0.089$ corresponds to a single N-N bonding.

Its counterpart $[\text{HN}\equiv\text{N}]^-$ has a N-N distance of 1.242 Å and $q_{\text{BCP}}(\text{N-N}) = 0.48$ e/bohr³ which correspond to the double N-N bond in contradiction with the too low $\epsilon_{\text{BCP}}(\text{N-N}) = 0.072$.

N₂ has a N-N distance of 1.096 Å, $Q_{BCP}(N-N) = 0.714 \text{ e/bohr}^3$ and $\epsilon_{BCP}(N-N) = 0.000$ which is typical for the triple bond.

Finally, H₂N-N=NH with N-N distances of 1.36 and 1.24 Å, $Q_{BCP}(N-N)$ values of 0.37 and 0.48 e/bohr³ as well as $\epsilon_{BCP}(N-N)$ values of 0.23 and 0.13, respectively, probably correspond to nearly double N-N bonds.

The F(11)(22) system is explained within the HN=NH and H₂N-NH₂ structures above.

The F12)(21 structure (aside from different numbering of N atoms) corresponds to the D2112 structures explained above.

We have not discussed N-H bonding in the systems under study because of the too small differences in their bond lengths and BCP electron densities. However, their BCP electron densities are higher than those of N-N bonds except HN=NH, H₂N=N, [HN=NH]⁺ and N₂. Increased $\epsilon_{BCP}(N-H)$ values can be ascribed mostly to a double bond character of neighboring N-N bonds, except $\epsilon_{BCP}(N-H) = 0.3$ in NH₃ molecules within the E(3)(102) systems.

The nitrogen atomic charges in the A and D structures (Table 9) are more negative on the N1 and N4 atoms (-0.65 to -0.82) than on the central N2 and N3 atoms (-0.35 to -0.50). Positive hydrogen atomic charges bonded to side N1 and N4 atoms increase with the number of bonded H atoms. The same trend holds for H atoms bonded to central N2 and N3 atoms which are more positive than the side hydrogens. **Table 9.** Atomic charges of N and H (bonded to N in brackets) in the optimized Amnpq and Dmnpq structures. The asterisks denote the atoms included in hydrogen bonds as well.

Structure	N1	N2	N3	N4	H(N1)	H(N2)	H(N3)	H(N4)
D1221	-0.657	-0.488	-0.485	-0.649	0.342	0.452 0.455	0.444 0.457	0.342
D2112a	-0.699	-0.347	-0.367	-0.706	0.379 0.392	0.391	0.382	0.391 0.404
D2112b	-0.691	-0.357	-0.354	-0.726	0.378 0.394	0.372	0.395	0.387 0.398
D2112c	-0.711	-0.354	-0.368	-0.729	0.377 0.389	0.382	0.396	0.389 0.401
D2121a	-0.700	-0.341	-0.398	-0.787	0.394 0.413	0.417	0.452(2×)	0.309
D2121b	-0.704	-0.361	-0.394	-0.811	0.400 0.416	0.405	0.470 0.560	0.302
D2121c	-0.709	-0.365	-0.412	- 0.800*	0.396 0.407*	0.406	0.463 0.468	0.310
D2121d	-0.707	-0.361	-0.395	-0.809	0.402 0.420	0.408	0.458 0.471	0.304
A2202	-0.664	-0.388	-0.435	-0.750	0.418(2×)	0.450(2×)	-	0.362(2×)
D2202a	-0.712	-0.404	-0.430	-0.760	0.409 0.410	0.455 0.475	-	0.361 0.364
D2202b	-0.705	-0.397	-0.432	-0.737	0.407 0.411	0.459 0.465	-	0.357 0.367
D2022	-0.761	-0.430	-0.402	-0.711	0.361 0.365	-	0.455 0.475	0.409 0.410
A3021	-0.730	-0.368	-0.388	-0.824	0.460	-	0.403	0.286

					0.461		0.423	
					0.496			
D3012a	-0.732	-0.436	-0.390	-0.739	0.449(2×)	-	0.370	0.360
					0.472			0.372
D3012b	-0.762	-0.417	-0.384	-	0.444	-	0.345	0.376
				0.754*	0.466*			0.378
					0.473			

In the decomposed E systems (Table 10), negative N charges increase with the number of bonded H atoms. An analogous trend for positive H charges cannot be confirmed. Atomic charges are only slightly affected by hydrogen bonding. In the E(32)(10) system, the charges of its [NH₃-NH₂]⁺ and [HN≡N]⁻ subsystems are +0.97 and -0.68, respectively. When the error of the electron density over atomic basins, the alternative biradical structure of the neutral E(32)(10) subsystems seems to be less probable.

Table 10. Atomic charges of N and H (bonded to N in bracket) in the optimized Emnpq and Fmnpq systems. Asterisks denote atoms included in hydrogen bonds as well.

System	N1	N2	N3	N4	H(N1)	H(N2)	H(N3)	H(N4)
E1111 ^{a)}	-0.345	-0.367*	-0.373	-0.367	0.383	0.408	0.396*	0.403
E(22)(11)a	-0.707	-0.727h	-0.358	-0.348*	0.380	0.385	0.409*	0.380
					0.392h	0.393		
E(22)(11)b	-0.727*	-0.707	-0.360	-0.348*	0.384	0.380	0.409*	0.380
					0.393	0.388*		
E(22)(11)c	-0.726*	-0.706	-0.349h	-0.360	0.384	0.380	0.380	0.409h
					0.393	0.387*		
E(22)(11)d	-0.706	-0.726h	-0.359	-0.347*	0.380	0.384	0.409*	0.380
					0.388h	0.393		
E(22)(20)a	-0.732*	-0.714	-0.519	-0.271*	0.380	0.387	0.417	-
					0.393*	0.395	0.460*	
E(22)(20)b	-0.713	-0.732*	-0.517	-0.273*	0.380	0.387	0.417	-
					0.393*	0.395	0.461*	
E(22)(02)	-0.714	-0.732*	-0.272*	-0.517	0.380	0.387	-	0.417
					0.393*	0.395		0.460*
E(31)(20)	-0.751	-0.831*	-0.543	-0.306*	0.447	0.315	0.408	-
					0.452		0.511*	
					0.491*			
E(32)(10)	-0.718	-0.731	-0.426	-0.530*	0.496	0.408	0.185	-
					0.508(2×)	0.501*		
E(3)(201)	-1.079*	-0.734	-0.035	-0.436	0.394(3×)	0.443	-	0.388
						0.473*		
E(3)(102)a	-1.076*	-0.454	-0.033	-0.686	0.394(3×)	0.428*	-	0.429
								0.445
E(3)(102)b	-1.084*	-0.396	-0.030	-0.739	0.394	0.352	-	0.445

					0.395			0.470*
					0.396			
E(3)(00)(3)	-1.077*	0.076*	-0.049	-1.059	0.382	-	-	0.373
					0.382*			0.380*
					0.384			0.386
F(11)(22)	-0.359	-0.347h	-0.706	-0.725*	0.409h	0.380	0.380	0.393
							0.388*	0.394
F12)(21 ^b)	-0.356	-0.722	-0.702	-0.368	0.403	0.377	0.371	0.381
						0.392	0.395	

3. Method

Geometry optimizations of various isomers of neutral N₄H₆ molecules were performed at the CCSD (Coupled Cluster using Single and Double substitutions from the Hartree-Fock determinant) [10] level of theory and cc-pVTZ basis sets [11]. The effects of the aqueous solution were taken into account within the SMD (Solvation Model based on the solute electron Density) solvation model [12]. The optimized structures were tested by vibrational analysis on the absence of imaginary vibrations. Gaussian16 (Revision B.01) software [13] was used for all quantum-chemical calculations.

The electron structure of the systems under study was evaluated in terms of Quantum Theory of Atoms-in-Molecules (QTAIM) [9] using AIM200 software [14]. The bond strengths were compared according to the electron densities ρ at the bond critical points (BCP). The BCP bond ellipticities ϵ_{BCP} were evaluated as

$$\epsilon_{BCP} = \lambda_1/\lambda_2 - 1 \tag{6}$$

where λ_i are the eigenvalues of the Hessian of the BCP electron density within the sequence $\lambda_1 < \lambda_2 < 0 < \lambda_3$. Atomic charges were obtained by integration over atomic basins up to 0.001 e/bohr³.

Visualization and geometry modification were performed using MOLDRAW software (<https://www.moldraw.software.informer.com>, accessed on 9 September 2019) [15].

4. Conclusions

We have shown that most N₄H₆ structures in aqueous solutions are decomposed during geometry optimization. Splitting the bond between central nitrogen atoms is the most frequent, but the breakaway of the side nitrogen is energetically the most preferred. The N-N fissions are enabled by suitable hydrogen rearrangements. The initial H₂N-NH-NH-NH₂ structure (D2112) has a very weak central N-N bond, which explains the high degree of reversibility of the reaction (5). The most stable system NH₃...N₂...NH₃ (E(3)(00)(3) system) might be obtained by transfers of both H atoms bonded with central nitrogens to the side N atoms. According to [8], such double H transfer was not found by quantum-chemical calculations in vacuo, and must be decomposed into several steps and this instantaneous decomposition should be slowed down. Furthermore, our calculations show that the transfer of the third H atom to the side nitrogen is very energetically disadvantageous, as indicated by the Gibbs energies of the structures NH₃-N = NH₂-NH and NH₃-N = NH-NH₂ (A3021 and D3012, respectively, see Table 2). In aqueous solutions, H atom transfers can be mediated by H₂O, H₃O⁺ and/or OH⁻ species. We have shown that side N atoms have very high negative charges that should support such hydrogen transfers.

The experimentally observed formation of ¹⁵N¹⁴N molecules [1–4] is enabled by side N-N fissions. We have shown that the Gibbs free energy data (Table 2) indicate the dominant abundance of NH₃... N₂... NH₃ species (E(3)(00)(3) system) in aqueous solutions, which explains the mentioned observations.

The ¹⁵N¹⁴N molecules can also be created by the decomposition of cyclic N₄H₆ structures. We have shown a high instability of such species. The only stable cyclo-(NH)₄...H₂ structure (E1111) has

a too high Gibbs energy and breaks the H₂ molecule instead. The remaining initial cyclic structures are split into hydrazine and HN≡NH (E(22)(11)d) or H₂N≡N species (E(22)(02), see Table 2) and their relative abundance in aqueous solutions is vanishing.

We can deduce from the QTAIM analysis of our systems that single, double and triple N-N bonds exhibit BCP electron densities of ca 0.2, 0.5 and 0.7 e/bohr³ with BCP ellipticities of ca 0, 0.2 and 0, respectively. The bonds in the N₄H₆ structures often exhibit significant deviations from these values.

Our study did not solve all problems related to hydrazine oxidation in aqueous solutions. The role of various water forms and the corresponding transition states should also be investigated. An alternative reaction pathway through N₄H₄ [6] according to reaction (4) is worth a study as well. Further theoretical studies in these fields are desirable.

Author Contributions: Methodology, software, investigation, writing—original draft preparation, writing—review and editing, M.B.; conceptualization, supervision, project administration, funding acquisition, A.M. All authors have read and agreed to the published version of the manuscript.

Funding: This publication was supported by the Competence Center for SMART Technologies for Electronics and Informatics Systems and Services, ITMS 26240220072.

Institutional Review Board Statement: Not applicable.

Informed Consent Statement: Not applicable.

Data Availability Statement: All necessary research data are presented in the article.

Acknowledgments: The authors thank the HPC center at the Slovak University of Technology in Bratislava, which is a part of the Slovak Infrastructure of High Performance Computing (SIVVP Project No. 26230120002, funded by the European Region Development Funds), for computing facilities.

Conflicts of Interest: The authors declare no conflict of interest.

Sample Availability: Not applicable.

References

1. Lauko, L.; Hudec, R.; Lenghartova, K.; Manova, A.; Cacho, F.; Beinrohr, E. Simple Electrochemical Determination of Hydrazine in Water. *Pol. J. Environ. Stud.* **2015**, *24*(4), 1659-1666
2. Higginson, W. C. E.; Sutton, D. The Oxidation of Hydrazine in Aqueous Solution. Part II. The Use of ¹⁵N as a Tracer in the Oxidation of Hydrazine. *J. Chem. Soc.*, **1953**, 1402-1406.
3. Cahn, J. W.; Powell, R. E. Oxidation of Hydrazine in Solution. *J. Am. Chem. Soc.*, **1954**, *76*, 2568-2572.
4. Petek, M.; Bruckenstein, S. An Isotopic Labeling Investigation of the Mechanism of the Electrooxidation of Hydrazine at Platinum. An Electrochemical Mass Spectrometric Study. *Electroanal. Chem. Interrac. Electrochem.* **1973**, *47*, 329-333.
5. Rice, F. O.; Sherber, F. The Hydrazino Radical and Tetrazane. *J. Am. Chem. Soc.* **1955**, *77*, 291-293
6. Karp, S.; Meites, L. The Voltammetric Characteristics and Mechanism of Electrooxidation of Hydrazine. *J. Am. Chem. Soc.* **1962**, *84*, 906-912.
7. Ball, D. W. Tetrazane: Hartree-Fock, Gaussian-2 and -3, and Complete Basis Set Predictions of Some Thermochemical Properties of N₄H₆. *J. Phys. Chem. A* **2001**, *105*, 465-470.
8. Dana, A. G.; Moore III, K. B.; Jasper, A. W.; Green, W. H. Large Intermediates in Hydrazine Decomposition: A Theoretical Study of the N₃H₅ and N₄H₆ Potential Energy Surfaces. *J. Phys. Chem. A* **2019**, *123*(22), 4679-4692.
9. Bader, R. F. W. *Atoms in Molecules: A Quantum Theory*. Clarendon Press, Oxford, U.K., 1990. ISBN: 9780198558651
10. Scuseria, G. E.; Janssen, C. L.; Schaefer III, H. F. An efficient reformulation of the closed-shell coupled cluster single and double excitation (CCSD) equations. *J. Chem. Phys.* **1988**, *89*, 7382-7387.
11. Dunning Jr., T.H. Gaussian basis sets for use in correlated molecular calculations. I. The atoms boron through neon and hydrogen. *J. Chem. Phys.*, **1989**, *90*, 1007-1023.
12. Marenich, A. V.; Cramer, C. J.; Truhlar, D. G. Universal solvation model based on solute electron density and a continuum model of the solvent defined by the bulk dielectric constant and atomic surface tensions. *J. Phys. Chem. B* **2009**, *113*, 6378-6396.

13. Frisch, G.W.M.J.; Schlegel, B.; Scuseria, G.E.; Robb, M.A.; Cheeseman, J.R.; Scalmani, G.; Barone, V.; Petersson, G.A.; Nakatsuji, H.; Li, X.; et al. *Gaussian 16, Revision B.01*; Gaussian, Inc.: Wallingford, CT, USA, 2016.
14. Biegler-König, F.; Schönbohm, J.; Bayles, D. AIM2000 —A Program to Analyze and Visualize Atoms in Molecules. *J. Comput. Chem.* **2001**, *22*, 545-559.
15. Ugliengo, P. MOLDRAW: A Program to Display and Manipulate Molecular and Crystal Structures, University Torino, Torino. 2012. Available online: <https://www.moldraw.software.informer.com> (accessed on 9 September 2019).

Disclaimer/Publisher's Note: The statements, opinions and data contained in all publications are solely those of the individual author(s) and contributor(s) and not of MDPI and/or the editor(s). MDPI and/or the editor(s) disclaim responsibility for any injury to people or property resulting from any ideas, methods, instructions or products referred to in the content.